Principle of Focus Shift for a Microscope Objective BONZ (NS-310B)

David Meijvogel
Student number 3836037
Utrecht University

June 13, 2014

Supervisor: Dr. Sasha Agronskaia

Abstract

In this research I investigated an optical system of a microscope objective and an imaging lens. This project is a small part of the project: "Integrated super-resolution correlative microscopy". The main goal for this project is to build a fluorescence wide-field microscope with photo-activated localization microscopy (PALM) capability inside a commercial transmission electron microscope (TEM). In order to gain room inside the limited space of the TEM column, I need to know how to optimize the optical system. I have found formulas which predict the position of the objective relative to the sample and the relative magnification (and therefore magnification).

1 Introduction

1.1 The Research

In this research I investigated how a multiple lenses system works. A microscope objective is used in the system. I want to predict how the objective along with an imaging lens will work. The purpose is to manipulate the focal distance of the system without losing the quality of imaging.

This information is relevant for building a microscope where wide field microscopy and transmission electron microscopy (TEM) are combined. The wide field microscope will have the ability to use photo-activated localization microscopy (PALM). TEM has the disadvantage that locating the interesting area is hard to determine. Combining the two mentioned techniques (TEM and PALM) should complement each other.

With the normal fluorescence microscopy (resolution 200 nm)(Na Ji et al. 2008), you can look for the region of interest, with PALM (resolution 10 nm)(Betzig et al. 2006) you can get a higher resolution and with TEM (resolution 4 nm)(Baumeister 2002) the desired resolution for studying biological samples is achieved. Prior to building the objective in the microscope, I want to know in what way I can manipulate the optical system. I want to have as much space as possible between the objective and the sample we are looking at. How much space can I gain and how does that effect the quality of the images? To be able to answer these questions it is handy to know how a multiple lenses system, involving the objective, works. In section 2 I describe the methods I used and how I prepared the sample, in section 3 I show the results I got and in section 4 I will discuss the results.

1.2 What is TEM?

"A modern TEM is composed of an illumination system, the magnification system, the data recording system(s), and the chemical analysis system"(Wang et al. 2000). Though, a chemical analysis system is not always present. A schematic graph of a transmission electron microscope can be seen in figure 1.

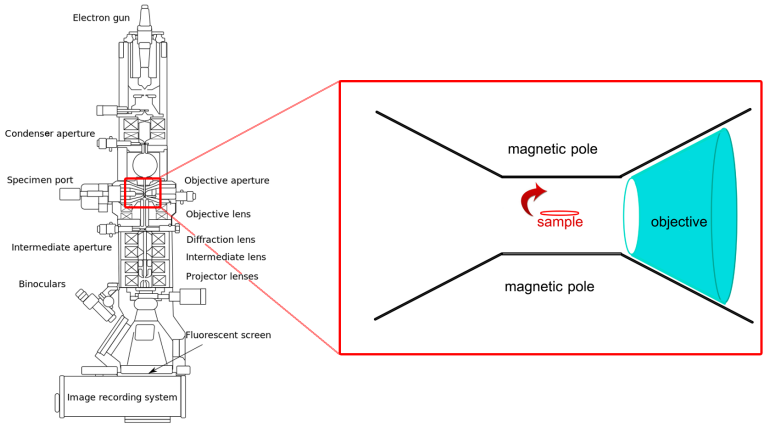

Figure 1: A Schematic graph of an electron microscope

In this figure the illumination system consists of the electron gun and the condenser aperture. The magnification system consists of the objective aperture, objective lens, diffraction lens, intermediate lens and the projector lens. The data recording systems consist of the fluorescent

screen and the image recording system. The chemical analysis system is usually placed outside, and coupled with, the microscope.

The specimen gets shot by the electron gun. The condenser-lens system allows variation of the illumination aperture and the area of the specimen illuminated. After the electrons hit the specimen, you get an electron intensity distribution. This distribution is projected, with the magnification system, onto a fluorescent screen. "The image can be recorded by direct exposure of a photographic emulsion or an image plate inside the vacuum, or digitally via a fluorescent screen coupled by a fiber-optic plate to a CCD camera"(Reimer and Kohl. 2008). These devices are part of the data recording systems. Our microscope will find its application in the biology, so we will focus on constructing images with the recorded data.

In figure 1 we see the red squared part of the electron microscope magnified. The sample holder is able to rotate. The position in which it is sketched is for the use of the electron microscopy and for using PALM microscopy it must rotate 90 degrees. As can be seen in figure 1, the magnetic poles limit the space to mount the objective at the correct distance from the sample (according to the mechanics drawings the objective can be just fitted at its working distance). Modern objectives with very long working distance and moderate NA can be fitted behind the magnetic poles(Iijimaa et al. 2014). However, the question remains if I can get an objective with reasonably high NA (0.55) to be positioned close enough to the sample in order to work properly.

1.3 What is PALM?

Nowadays there are a lot different forms of super-resolution microscopy. For example STED (stimulated emission depletion)(Hell 2003), STORM (stochastic optical reconstruction microscopy) (Rust et al. 2006) or PALM (photo-activated localization microscopy)(Betzig et al. 2006). I will take a closer look at PALM.

In microscopy there is a limit to what resolution you can get. We can't infinitely zoom in on particles. If particles fluorescence you can see them as point sources. At a certain moment you can't distinguish two different point sources. This limit is given by the Rayleigh Criterion(Garini et al. 2005).

$$r_R = 0.61\frac{\lambda}{NA}$$

where λ is the wavelength of the detected photons and NA is the numerical aperture of the lens system. This is the limit on resolution of point sources imposed by the finite size of the diffraction-limited illumination volume in a far-field optical system (Hess et al. 2006). This means that you can't see two separate point sources close to each other, instead you would see one blurry light dot. If you can exceed the Rayleigh limit in microscopy, it is called super-resolution(Schermelleh et al. 2010). PALM deceives this limit.

With PALM you first illuminate your sample with an activation laser. This laser makes the subset of particles capable to fluorescence. The chance that two particles, that are separated by less than the Rayleigh limit, are activated at the same time is relative small. Mostly the wavelength of this laser is $\lambda_{act} = 405$ nm. Then you excite our sample with an excitation laser, this laser causes the activated particles to emit or fluorescence. This fluorescence can be detected and thus particles can be localized. The particles bleach (stop emitting) after a certain time, so you want to locate as many particles as possible within this time because after being bleached, you can't locate the particles again. This means a lower quality of localization. This is where one cycle ends. The cycle is repeated many times, over 10^4 times(Betzig et al. 2006). Locations for other particles are revealed per cycle. For completing the super-resolution image, all the images

from different cycles get stacked. The process of stacking can be seen in the vertical direction and the process of particle localization in the horizontal direction, in figure 2.

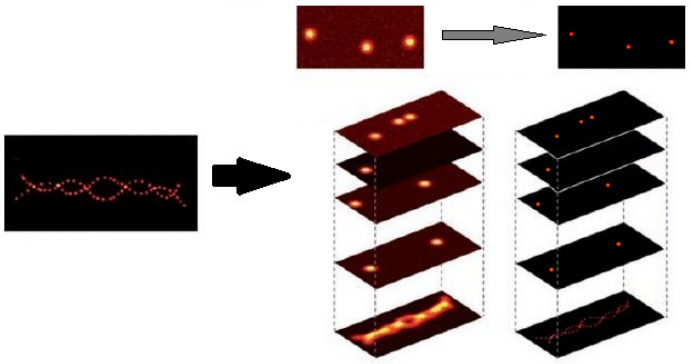

Figure 2: PALM process, particle localization and stacking

After stacking the different images you can transcend the Rayleigh limit.

2 Methods

I, with colleagues, build a homemade wide field fluorescence microscope (see figure 3). The green beam is the beam coming from the laser (*New Focus* laser with a wavelength of 532 nanometer, serial number 030922161). The laser beam is spatially cleaned by a diaphragm. Next, the laser beam is expended 10 times by two lenses with focal lengths of -10 mm and 100 mm and focused to the back aperture of the Nikon objective (CF IC EPI Plan ELWD , NA 0.55, 50x, air) by an achromatic lens of 300 mm (Köhler illumination). The (green) beam arrives at the objective via the dichroic mirror. The beam (out of the objective) hits the sample (orange latex beads with 0.2 micrometer diameter), which is mounted on a Piezo stage (P-611.Z Piezo Z-stage), and the fluorescence goes back through the objective. The sample is placed around the focal distance of the objective to get a clear image. The orange beam goes through the dichroic mirror, through the emission filter (RazorEdge, Long Pass 532.0) and through an imaging lens (with $f = 300$ mm, but I varied this lens with lenses of $f = 200$ mm and $f = 100$ mm) which focuses the image at the camera (a sCMOS pco.edge 4.2 camera). The camera is connected to a computer which makes images of the sample with software that is delivered with the camera.

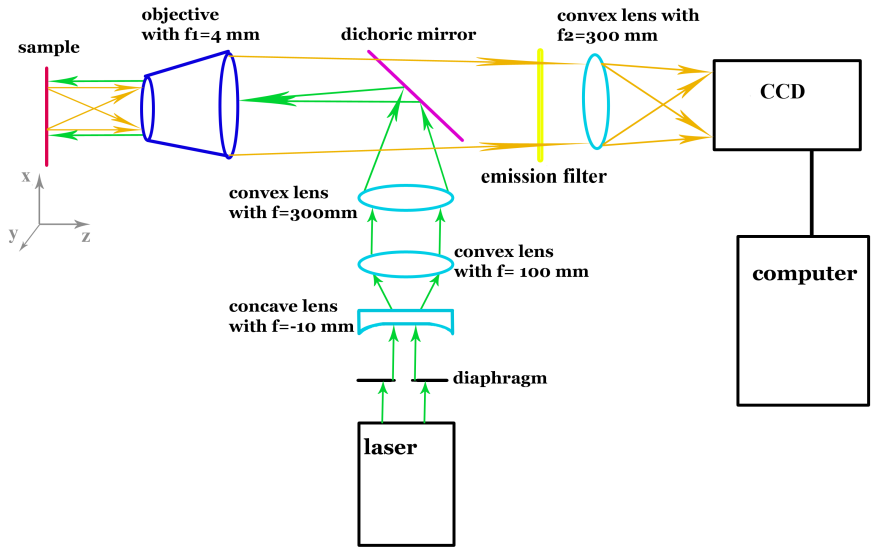

Figure 3: setup for second experiment

For the objective a stable movable mount is needed. The positioning of the objective had some last subtle adjustments to get it exactly in place. The sample will needed a stable mount which is able to move in three dimensions. I made the sample holder with x, y and z mechanical stages and a Piezo Z-stage. The z direction is for focusing and the x and y directions are used to trace the same area on the sample for every time the camera is moved to a different position. With the Piezo stage, I can move our sample in the order of micrometers. At last, the dichroic mirror must be able to be adjusted, including the angle. The dichroic mirror must have an angle of exact 45 degrees with respect to the laser beam and it has to be perpendicular to the table, this way the laser beam keeps the same height. Focal lengths are given in mm. I analyzed the data with *ImageJ* and did the calculations with *Mathematica*.

2.1 Sample Preparation

I used orange latex beads with 0.2 micrometer diameter as a sample. I diluted this 1:800 with water. I put a droplet of 2 μL of the sample on a (standard) microscope slide from Menzel-Gläser (76x26 mm). Then I let the sample slowly evaporate and placed it on a Piezo stage.

2.2 Focus shift

A simplified image of the situation can be seen in figure 4. Here you see that the beam focuses in between the objective and the imaging lens. This is not true in the real situation, but I use this to make clear what I mean with s_1' and s_2'.

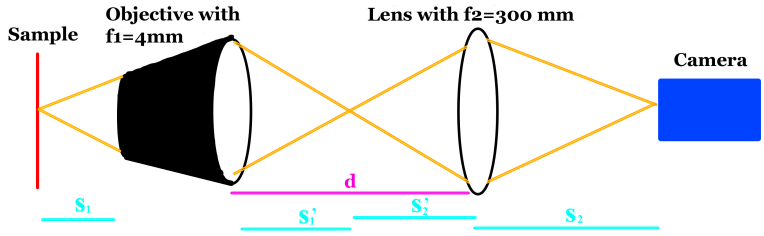

Figure 4: Simplified situation for experiment

In the figure s_1 is the distance between the objective and the sample, s_1' is the distance from the objective to the focus in between (the objective and imaging lens), s_2' is the distance from the focus in between to the second lens, s_2 is the distance from the second lens to the camera and d (d=362±2 mm for $f_2 = 100$ mm and d=308±2 mm for $f_2 = 200$ mm and $f_2 = 300$ mm) is the distance between the objective and the imaging lens. I vary s_2 between 50 and 350 mm.

I found a formula to predict s_1 if I know s_2. I calculated the theoretical predication formula from simple geometry. From figure 4 follows $d = s_1' + s_2'$. I can express s_1' in s_1 and f_1. This principle is applicable to s_2' as well.

$$\frac{1}{f_1} = \frac{1}{s_1} + \frac{1}{s_1'} \rightarrow s_1' = \frac{1}{\frac{1}{f_1} - \frac{1}{s_1}}$$

$$\frac{1}{f_2} = \frac{1}{s_2} + \frac{1}{s_2'} \rightarrow s_2' = \frac{1}{\frac{1}{f_2} - \frac{1}{s_2}}$$

I substitute these in the equation for d and after simplifying I get equation 1.

$$d = s_1' + s_2' = \frac{1}{\frac{1}{f_1} - \frac{1}{s_1}} + \frac{1}{\frac{1}{f_2} - \frac{1}{s_2}} = \frac{f_1 s_1}{s_1 - f_1} + \frac{f_2 s_2}{s_2 - f_2} \tag{1}$$

I want to express s_1 in terms of s_2. This way I can predict where I have to put the sample if I know the distance between the imaging lens and the camera.

$$(s_1 - f_1)d - f_1 s_1 = ds_1 - f_1 s_1 - df_1 = \frac{(s_1 - f_1) f_2 s_2}{s_2 - f_2} = \frac{s_1 f_2 s_2}{s_2 - f_2} - \frac{f_1 f_2 s_2}{s_2 - f_2}$$

$$ds_1 - f_1 s_1 - \frac{s_1 f_2 s_2}{s_2 - f_2} = s_1 \left(d - f_1 - \frac{f_2 s_2}{s_2 - f_2} \right) = df_1 - \frac{f_1 f_2 s_2}{s_2 - f_2}$$

From this follows equation 2.

$$s_1 = \frac{df_1 - \frac{f_1 f_2 s_2}{s_2 - f_2}}{d - f_1 - \frac{f_2 s_2}{s_2 - f_2}} = \frac{df_1(s_2 - f_2) - f_1 f_2 s_2}{(d - f_1)(s_2 - f_2) - f_2 s_2} \tag{2}$$

If I take $s_2 = f_2$, then s_1 should be f_1. If $s_2 = f_2$, it means that the beam that is incoming in the lens with f_2 is parallel, according to the laws of geometrical optics. The only way a parallel beam is produced, is when the sample is placed exactly at $s_1 = f_1$. Filling in $s_2 = f_2$ gives

$$s_1 = \frac{df_1(f_2 - f_2) - f_1 f_2 f_2}{(d - f_1)(f_2 - f_2) - f_2 f_2} = \frac{-{f_2}^2 f_1}{-{f_2}^2} = f_1$$

This is correct. I will hold formula 2 as the theoretical prediction of s_1.

The order of formula 2 will not be the same as the formula I fit on the obtained data, since I used a thin lens approximation ($\frac{1}{f_2} = \frac{1}{s_2} + \frac{1}{s_2'}$), while I have an objective which I absolutely can't see as a thin lens. Therefore I only care about the compatibility of the shape of the curve of formula 2.

To measure the distance s_1 between the sample and the objective (when the camera was moved to a distance s_2), I used the Piezo stage. Before using the Piezo stage, I moved the sample in place with a mount with an uncertainty of 1 mm. I determined the value for s_1 (before using the Piezo stage) with calculating the difference between the sample in focus and the sample in touch with the objective. The sample is prepared on a microscope slide, this microscope slide is able to bend a little bit. Therefore it is harder to determine when the sample touches the objective exactly. This way the uncertainty in the mechanical stage increases and I found different orders in s_1 for different values of f_2.

The uncertainty in s_2 is $\sigma_{s_2} = 1.5$ mm. I measured this distance with a ruler, the uncertainty is based on the use of this ruler. The uncertainty in s_1 is $\sigma_{s_1} = 4$ μm, this number is based on a clear sight of where the focus was in combination with the accuracy of the Piezo stage. The uncertainty in d is $\sigma_d = 2$ mm. The uncertainty in d is slightly more than σ_{s_2} because the uncertainty in d was harder to read than σ_{s_2}. It was harder to read because the dichroic mirror was placed in between the objective and the imaging lens.

2.3 Magnification

2.3.1 Recognizable areas

For determining the magnification I have drawn lines in every image (with different s_2-position) between the same two recognizable beads. I measured the length of the lines in pixels in *ImageJ*. I made sure that I drew long lines, this way I decrease our uncertainty, from the centre of the beads.

I divided the length of every line by the length of the line measured at $s_2 = f_2$, this way I get the relative magnification. To get the absolute magnification I multiply the relative magnification by f_2/f_1. The uncertainty in the length of the line I estimate at 6 pixels. This number is based on the certainty that I was in the centre of a bead. When the length of the line at $s_2 = f_2$ was unknown, I first fitted a line through the obtained data. This way I get a function which predicts the length of the line (in pixels) depending on s_2. In this function I filled in $s_2 = f_2$ to get the length that the line supposed to be at $s_2 = f_2$.

I expressed the numbers from the fit (of the relative magnification) in the variables the optical system (see figure 4) f_1, f_2 and d. In combination with the boundary condition that $M_R = 1$ when $s_2 = f_2$, I got the formula for the relative magnification.

I combined $\sigma_\alpha = |\sigma_{\alpha_1}| + |\sigma_{\alpha_2}| + ... + |\sigma_{\alpha_N}|$, when N quantities are summed, and $\frac{\alpha}{|\sigma_\alpha|} = \frac{\alpha_1}{|\sigma_{\alpha_1}|} + \frac{\alpha_2}{|\sigma_{\alpha_2}|} + ... + \frac{\alpha_N}{|\sigma_{\alpha_N}|}$, when N quantities are multiplied, to determine the uncertainty in the relative magnification.

2.3.2 Non recognizable areas

I assume that the beads are heterogeneously distributed for the different images. With this assumption made, I measured several distances between y-coordinates (y-direction is the vertical direction) of neighboring beads. This vertical direction is more accurate because the camera has less degrees of freedom in this direction (it was easier the rotate than tilt the camera). I measured the average neighborhood vertical distance for each image (in pixels). This averaged value is a measure of the magnification of different images. I can determine with which factor the images are magnified relative to each other. If the uncertainty is to big (more than 10%) I can't quantify this factor, in that case I can only qualitative say if images are magnified relative to each other.

2.4 Quality

The 2D paraxial wide field fluorescence microscope point-spread function (WFFM PSF), or "Airy disk" (like figure 5, figures of Airy disks can be found all over the internet), describes the two-dimensional distribution of light in a focal plane for point sources. The 2D paraxial WFFM PSF can be approximated by Gaussian functions(Zhang et al. 2007). In this investigation I will hold the width of such an approximated Gaussian function as a benchmark for the quality.

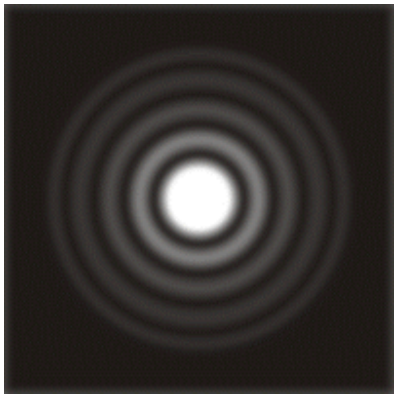

Figure 5: Airy disk

For the quality of images, I fitted 2D Gaussian functions on the fluorescence intensities of twelve beads. From these fitted Gaussian functions I determined the width. I took the average width of the 24 widths. This value is correlated with the quality of our pictures. In this case, the smaller the value, the better the quality. I estimated the uncertainty in the distance between the sample and the objective at 0.05 μm, this is based on the accuracy of the Piezo stage. The uncertainty for each averaged width is calculated using equation 3,

$$\sigma = \sqrt{\frac{1}{N}\sum_{i=1}^{N}(z_i - \mu)^2} \tag{3}$$

where $\mu = 1/N \sum_{i=1}^{N} z_i$, is the average value of z (of all the 24 widths) and z_i is the width of a Gaussian function.

To convert the width of a fitted Gaussian to a Rayleigh resolution, I multiply the width with 2.8991.... If I plot (see figure 6) a PSF with a Rayleigh radius of one ($r_R = 0.61\frac{\lambda}{NA} = 1$), the corresponding fitted Gaussian has a width of 0.34493.... This means I have multiply the width of the fitted Gaussian with 1/0.34493... = 2.8991... to convert the width to the Rayleigh resolution. As PSF function for this simplified plot, I used $PSF(x) = \left(2\frac{J_1(x)}{x}\right)^2$ (Zhang et al. 2007), with boundary condition $PSF(0) = 1$. Here J_1 is the first-order Bessel function of the first kind.

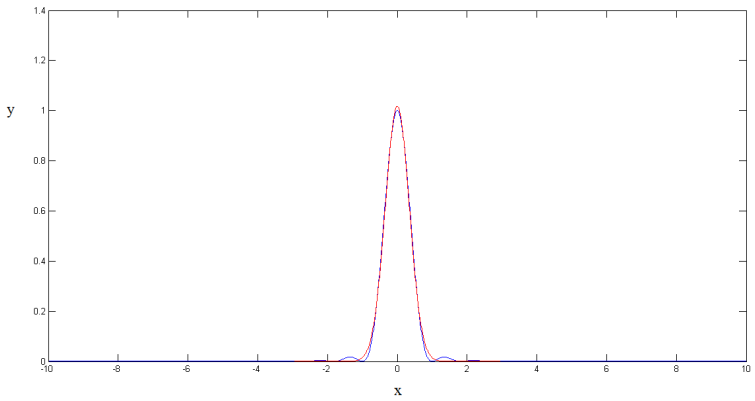

Figure 6: PSF(x) with $r_R = 1$ (blue) and corresponding fitted Gaussian with $\sigma = 0.34493$ (red)

3 Results

3.1 Focus shift

I measured the distance s_1 when the camera was place at a distance s_2 (see figure 4), then I compared this data with the theoretical prediction. I only looked at the shape of the curve (because of the thin lens approximation), so I lifted the curve (according to formula 2) with a certain number to investigate if the shape of the obtained data is compatible with the theoretical prediction. The results for $f_2 = 300$ mm and $f_2 = 200$ mm are given in figure 7. The theoretical prediction for $f_2 = 300$ mm is lifted 5.255 and for $f_2 = 200$ mm the curve is lifted 4.79. The difference in these numbers is so big because of the uncertainty in the mechanical stage (see Methods). The blue lines are the uncertainties in the theoretical prediction, coming from the uncertainty in d. The red line is the exact expectation curve. In figure 7 (a), the red line is hard to see because the uncertainties are small.

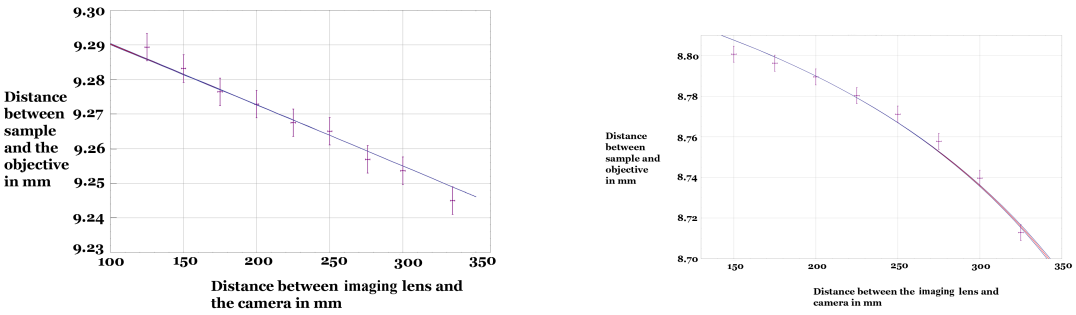

(a) $f_2 = 300$ mm

(b) $f_2 = 200$ mm

Figure 7: Found values and theoretical prediction for distance s_1

For $f_2 = 300$ mm, the shape matches. For $f_2 = 200$ mm, the shape seems to match. Only, not all the obtained data points correspond with the expectation curve. Also, the found values in the beginning are beneath the curve, slowly they grow above the curve, with exception of the last found value.

I also obtained data for $f_2 = 100$ mm. According to formula 2, there must be a pole at $(d - f_1)(s_2 - f_2) - f_2 s_2 = 0$. Working this out gives $s_2 = \frac{f_2(d-f_1)}{d-f_2-f_1} = 138.76 \pm 0.30$ mm. Therefore

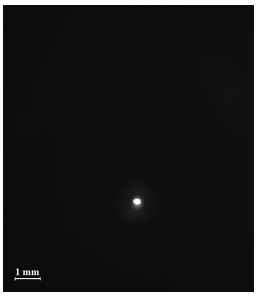

Figure 8: image made at $s_2 = 138 \pm 1.5$ mm for experiment 2, $f_2 = 100$mm

I made an image around this point. This image can be seen in figure 8. At this point most of the light is focused in one place. For this issue formula 2 predicts what we recorded.

Continuing with the focus shift. In purple is the obtained data from $50 < s_2 < 120$ and in pink is the data from $150 < s_2 < 220$. I lift the theoretical prediction for $50 < s_2 < 120$ with 4.61 and the theoretical prediction for $150 < s_2 < 220$ with 4.62. The results can be seen in figure 9.

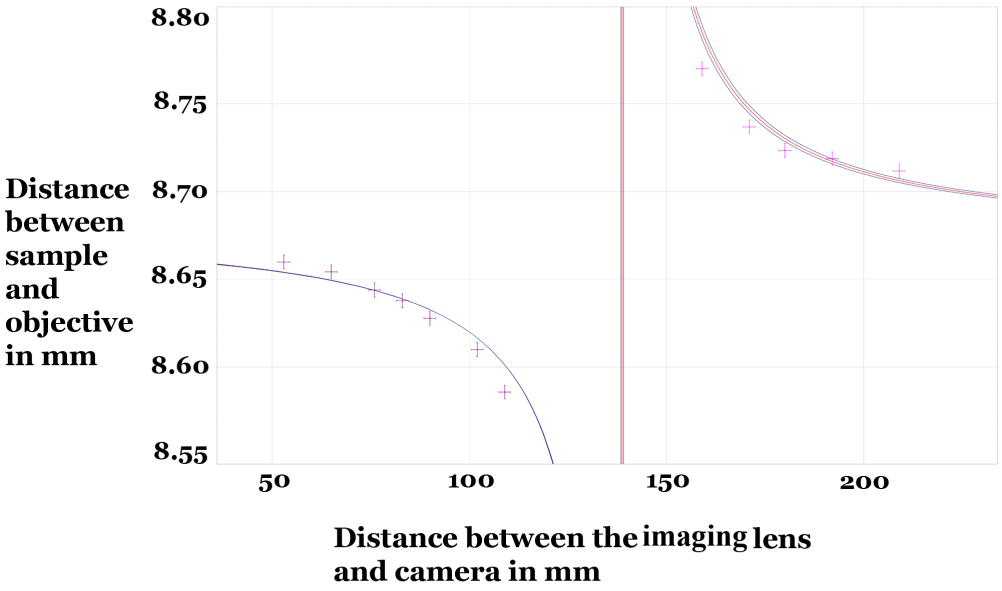

Figure 9: Found values and theoretical prediction for experiment 2, $f_2 = 100$ mm

The obtained values don't match really good with the expectation values, but they do have the same shape.

3.2 Magnification

I got the following formula for the magnification.

$$M_R = \left| \frac{d + f_1}{f_2} + \left(\frac{1}{f_2} - \frac{d + f_1}{f_2^2} \right) s_2 \right| \tag{4}$$

The obtained data with $f_2 = 300$ mm for the relative magnification can be seen, along with the curve of formula 4, in figure 10 (a). For $f_2 = 200$ mm the relative magnification can be seen, along with the curve of formula 4, in figure 10 (b). The blue curves are the uncertainties of formula 4, caused by the uncertainty in d ($\sigma_d = 2$ mm). The red curve is formula 4 with the measured d. This formula clearly corresponds with the obtained data perfectly.

For $f_2 = 100$ mm, the results are given in figure 11

Formula 4 doesn't perfectly correspond with the obtained data. Also the uncertainties are big. Although the uncertainties are quit big, the shape of the obtained data seems to have the

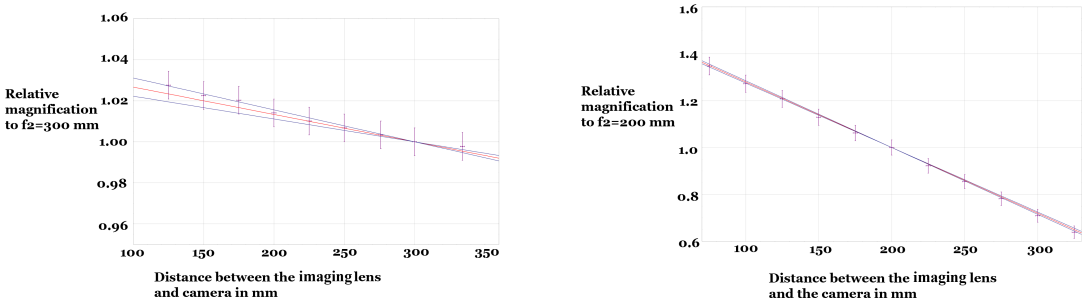

(a) $f_2 = 300$ mm (b) $f_2 = 200$ mm

Figure 10: Found values and formula for magnification

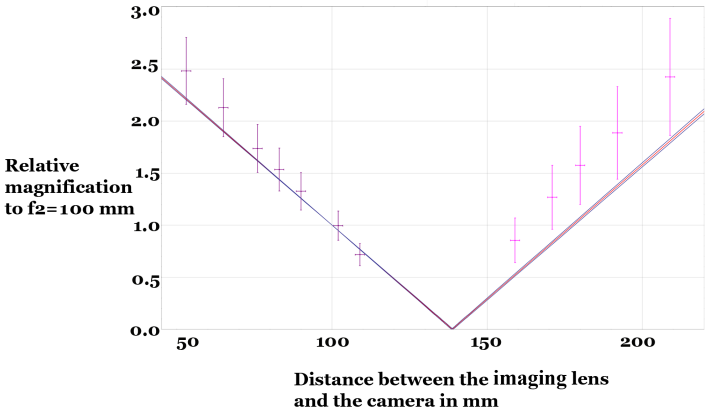

Figure 11: Found values and formula for magnification 2, $f_2 = 100$ mm

same shape as the curve of formula 4. Because the second data set ($150 < s_2 < 220$) is fully above the curve I measured the relative magnification also in a different way.

With a $f_2 = 100$ mm imaging lens, a relative magnification $M_R = 1$ is found at $s_2 = f_2 = 100$ mm and $s_2 = \frac{100(104+(362\pm2))}{-96+(362\pm2)} = 175.2 \pm 0.56$ mm (this means that a pixel is the same physical size at both s_2-values) according to formula 4. I checked if $M_R = 1$ at both places. At $s_2 = f_2$ this true anyway because this is the definition of the relative magnification (boundary condition: $s_2 = f_2 \rightarrow M_R = 1$), so I checked if the image at $s_2 = 175.2 \pm 0.56$ mm is equally magnified. I used a 1 mm reticle. This reticle is subdivided in sizes of 10 micrometers. I measured ten times 10 micrometers (in pixels) (see figure 12) and took the average, at both s_2-positions. These values I compared.

For $s_2 = f_2 = 100 \pm 1.5$ mm I found that 10 micrometers was 37.1 ± 1.2 pixels. At $s_2 = 175.2 \pm 1.5$ mm, 10 micrometers is 36.2 ± 3.7 pixels. One pixel size is 6.5 μm and 1 μm is 3.71 ± 0.12 pixels, so at $s_2 = 100 \pm 1.5$ mm I magnified $(3.71 \pm 0.12) \cdot 6.5 = 24.1 \pm 0.78$ times. This magnification differs only by 4% with the expected magnification($f_2/f_1 = 100/4 = 25$ times). From this it turns out that the relative magnification is indeed about one at both s_2-values.

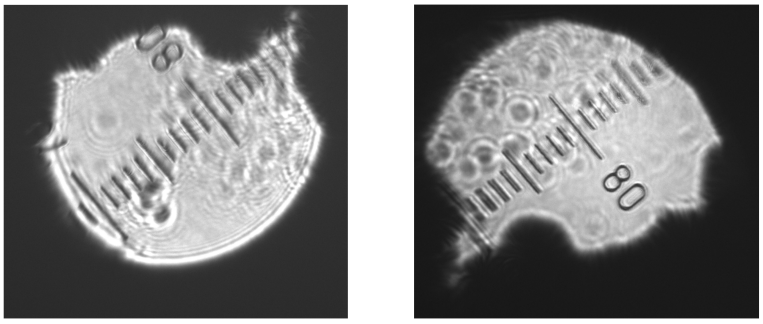

Figure 12: 1 mm reticle, $f_2 = 100$ mm

According to formula 2 I gain 0.128 ± 0.002 mm (between the sample and the objective) when the camera is positioned at $s_2 = 175.2 \pm 1.5$ mm.

3.3 Quality

Because the relative magnification seems to stay the same at $s_2 = 100 \pm 1.5$ mm and $s_2 = 175.2 \pm 1.5$ mm, I investigated the quality at both places. Since the width (in pixels) of fitted Gaussian will grow along with the relative magnification, I have to be absolutely sure that the $M_R = 1$ for the images at the both places. I couldn't find the same beads in the different images, so I applied the principle of distances between neighboring beads (see Methods). At $s_2 = 100 \pm 1.5$ mm I found an average value for the distance between neighboring beads in the vertical direction of 14 ± 11 pixels. At $s_2 = 175.2 \pm 1.5$ mm I found an average value for the distance between neighboring beads in the vertical direction of 25 ± 16 pixels. The uncertainties are to big to quantify a magnification factor between the two positions. It looks like the image at $s_2 = 175.2 \pm 1.5$ has a bigger magnification. However, the uncertainties are so enormous that I can't conclude that without having serious doubts.

Because I don't know for sure if the two s_2-positions have the same magnification, I looked at the illumination spot of the laser (see figure 13). I notice that the illumination spot at $s_2 = 175.2 \pm 1.5$ mm has a larger height h (in pixels) than at $s_2 = 100 \pm 1.5$ mm. Here I only look at the height, and not the width, because in this direction the camera has, as mentioned before, less degrees of freedom in the vertical direction. This points at a bigger magnification at $s_2 = 175.2 \pm 1.5$ mm than at $s_2 = 100 \pm 1.5$ mm. When analyzing, I take these doubts about magnification in count.

The averaged widths of the fitted Gaussians functions can be seen in figure 14. The focus for $s_2 = 100 \pm 1.5$ mm is at $s_1 = 9.1346 \pm 0.00005$ mm because at this position I find the lowest values for the averaged width of the fitted Gaussian functions. For $s_2 = 175.2 \pm 1.5$ mm, the focus is at $s_1 = 9.4296 \pm 0.00005$ mm. It is clear that extra space is gained between the sample and the objective, but the width of the fitted Gaussian functions at $s_2 = 175.2 \pm 1.5$ mm is almost twice the averaged width of fitted Gaussian functions at $s_2 = 100 \pm 1.5$ mm. Also, the uncertainties for the widths at $s_2 = 175.2 \pm 1.5$ mm are bigger.

Furthermore, the Rayleigh Criterion can be checked. For λ (emission wavelength) I take

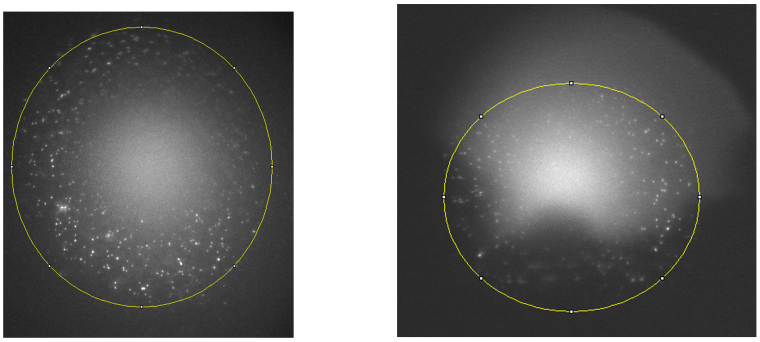

Figure 13: comparing illumination spots, $f_2 = 100$ mm

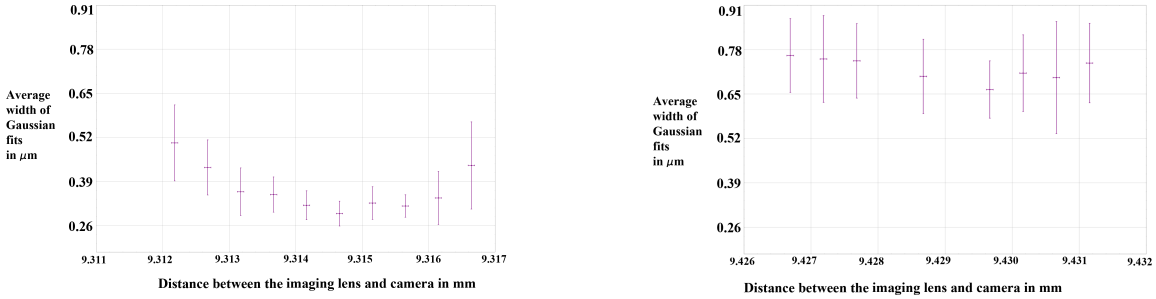

(a) $s_2 = 100 \pm 1.5$ mm

(b) $s_2 = 175.2 \pm 1.5$ mm

Figure 14: Width of Gaussian functions against position y.

570 ± 10 nm (orange) and $NA = 0.55$, so I get

$$r_R = 0.61\frac{\lambda}{NA} = 0.61\frac{(570 \pm 10) \cdot 10^{-9}}{0.55} = 0.63 \pm 0.01\mu m$$

The smallest width (thus in the focus) of the Gaussian fits I got at $s_2 = 100$ mm is 1.136 ± 0.141 pixels. One pixel is 6.5 μm and I magnified 25 times at this position, so the width is $(1.136 \pm 0.141) \cdot 6.5 \cdot 0.04 = 0.295 \pm 0.037$ μm. This width has to be transformed to the radius of a PSF, thus multiply by 2.8991. Thus the resolution I got is given by $(0.295 \pm 0.037) \cdot 2.8991 = 0.86 \pm 0.11$ μm. This means that the maximum resolution is well approached.

4 Discussion

I can discuss about the correctness of formula 2 for determining the position of the objective. The starting number has always been a mystery and, in the case of $f_2 = 100$ mm, the obtained values don't have a good match with what I expected. Now, because I have experimental obtained data that satisfies the theoretical predicted expectation at $s_2 = \frac{f_2(d-f_1)}{d-f_2-f_1}$ (see figure 8) and because the experimental obtained data has the same shape as the theoretical predicted expectation curve, I conclude that formula 2 is a good approximation.

The (relative) magnification, given by formula 4, seems to be correct for $f_2 = 300$ mm and for $f_2 = 200$ mm. However, for $f_2 = 100$ mm it has a few shortcomings. All the data points, but one, are found above the curve of formula 4. An extra argument wouldn't be misplaced. According to formula 4 the minimum is at $s_2 = \frac{f_2(d+f_1)}{d+f1-f_2}$. Comparing this with the minimum of 2 for position s_1, by filling in the numbers, gives

$$s_{2_{M_R}} = \frac{f_2(d+f_1)}{d+f1-f_2} = \frac{100((362 \pm 2)+4)}{(357 \pm 2)+4-100} = 137.59 \pm 0.28mm$$

$$s_{2_y} = \frac{f_2(d-f_1)}{d-f1-f_2} = \frac{100((362 \pm 2)-4)}{(357 \pm 2)-4-100} = 138.76 \pm 0.3mm$$

This is around the same point. Having this said, I conclude that formula 4 is very good approximation for the relative magnification for our system.

It is difficult to determine, from our data sets, what happens with the quality when s_2 is differed while M_R is the same (in theory, at $s_2 = f_2$ and $s_2 = 175.2 \pm 0.56$ mm). The main cause for this is that I am not sure about the magnification. According to the analysis of the reticle (see figure 12), the (relative) magnification is 2% bigger at $s_2 = 100 \pm 1.5$ mm than at $s_2 = 175.2 \pm 1.5$ mm. Taking the uncertainties in count, I could say that the (relative) magnification is the same at both places. However, analyzing the distance between neighbouring beads implies that the (relative) magnification at $s_2 = 175.2 \pm 1.5$ mm is bigger by a factor 1.79 than at $s_2 = 100 \pm 1.5$ mm, but the uncertainties are to big to confirm this factor without being suspicious. According to the analyzes of the illumination spot, the (relative) magnification is bigger at $s_2 = 175.2 \pm 1.5$ mm than at $s_2 = 100 \pm 1.5$ mm by a factor 1.17. Here I could question what exactly the illumination spot is and what determines its boundaries. What happens with the magnification is not clear. If it is the case of bigger magnification at $s_2 = 175.2 \pm 1.5$ mm, I would expect that the averaged widths of the fitted Gaussians are bigger at this s_2-value.

If the (relative) magnification is the same at both data sets, I could conclude that the quality drops when the camera is moved from $s_2 = 100 \pm 1.5$ mm to $s_2 = 175.2 \pm 1.5$ mm, because the averaged widths of the fitted Gaussian functions (which I hold as a benchmark for the quality) are bigger. If the (relative) magnification is bigger at $s_2 = 175.2 \pm 1.5$ mm, I can't conclude that the quality drops when the camera is moved from $s_2 = 100 \pm 1.5$ mm to $s_2 = 175.2 \pm 1.5$ mm, because the averaged widths of the fitted Gaussian functions would be growing along with the (relative) magnification, as expected. This means that the quality doesn't drop.

With formula 2 I can approximate where I have to put the camera to gain space between the sample and the objective. In combination with formula 4 I can determine how this positioning influences the magnification. If the quality doesn't drop to much (when applying the principle of focus shift), I might be able to gain more space. Still, I wouldn't be able to apply the principle of focus shift if the quality doesn't drop, because inside the microscope there is no space to move the camera the distance that is needed.

4.1 Future research

In future research, optical system with two lenses, which can be replaced by a virtual lens with focal length $f = \frac{f_1 f_2}{f_1+f_2-d}$ (see figure 15), and the validity of formula 2 and formula 4 could be investigated. This research would be fundamental research, so I can replace the objective with a

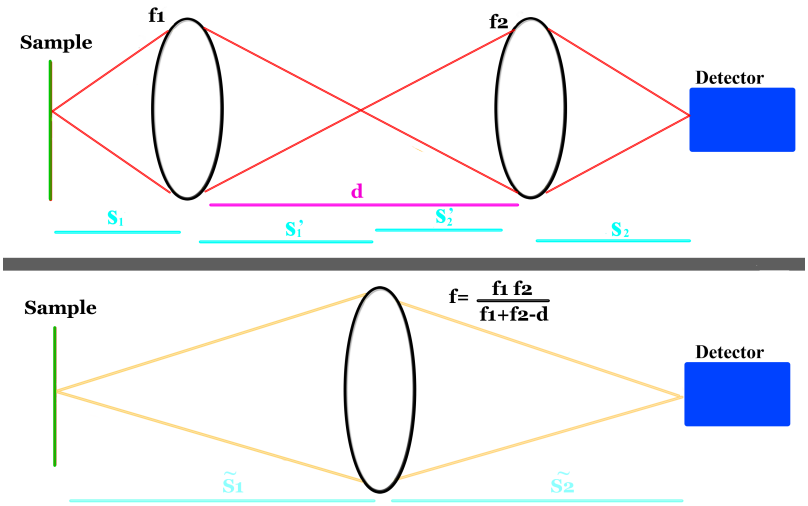

Figure 15: Schematic optical system

normal lens. If I would change formula 4 by replacing every $d + f_1$ with $d - f_1$, I get formula 5 for the relative magnification.

$$M_R = \left| \frac{d - f_1}{f_2} + \left(\frac{1}{f_2} - \frac{d - f_1}{f_2^2} \right) s_2 \right| \tag{5}$$

According to this formula the minimum is at $s_2 = \frac{f_2(d-f_1)}{d-f_1-f_2}$ and this is exactly the point where the pole of formula 2 is. The combinations of formula 2 and 5 could be the true formulas for an optical system with two lenses. Furthermore, I can determine $\tilde{s_1}$ and $\tilde{s_2}$ with these formulas. The magnification of a system as given in figure 15 is $M = \tilde{s_2}/\tilde{s_1}$ and the relative magnification by $M_R = (\tilde{s_2} f_2)/(\tilde{s_1} f_1)$. Also valid for such a system is

$$\frac{1}{f} = \frac{1}{\tilde{s_1}} + \frac{1}{\tilde{s_2}} \rightarrow \frac{\tilde{s_2}}{f} = \frac{\tilde{s_2}}{\tilde{s_1}} + 1 = \frac{f_1}{f_2} M_R + 1$$

If formula 5 is correct, I can substitute this formula so I get

$$\frac{\tilde{s_2}}{f} = \frac{f_1}{f_2} \left| \frac{d - f_1}{f_2} + \left(\frac{1}{f_2} - \frac{d - f_1}{f_2^2} \right) s_2 \right| + 1$$

Taking in count that $f = \frac{f_1 f_2}{f_1+f_2-d}$, I eventually get formula 6 for $\tilde{s_2}$.

$$\tilde{s_2} = \frac{f_1 f_2}{f_1 + f_2 - d} \left(\frac{f_1}{f_2} \left| \frac{d - f_1}{f_2} + \left(\frac{1}{f_2} - \frac{d - f_1}{f_2^2} \right) s_2 \right| + 1 \right) \tag{6}$$

If I again use $M = \tilde{s_2}/\tilde{s_1}$ and combine this with the expression for $\tilde{s_2}$ I can obtain a formula for $\tilde{s_1}$.

$$\frac{\tilde{s_2}}{\tilde{s_1}} = \frac{f_1}{f_2}\left|\frac{d-f_1}{f_2} + \left(\frac{1}{f_2} - \frac{d-f_1}{f_2^2}\right)s_2\right| = \frac{1}{\tilde{s_1}}\frac{f_1 f_2}{f_1+f_2-d}\left(\frac{f_1}{f_2}\left|\frac{d-f_1}{f_2} + \left(\frac{1}{f_2} - \frac{d-f_1}{f_2^2}\right)s_2\right| + 1\right)$$

Working this out gives

$$\tilde{s_1} = \frac{f_1 f_2}{f_1+f_2-d}\left(1 + \frac{1}{f_1}\frac{{f_2}^3}{|f_2(d-f_1)+(2f_2-d)s_2|}\right) \tag{7}$$

Summarized, future research could be done on the validity of formula 2, formula 5, formula 6 and formula 7 for an optical system with two lenses (see figure 15).

$$s_1 = \frac{df_1(s_2-f_2) - f_1 f_2 s_2}{(d-f_1)(s_2-f_2) - f_2 s_2}$$

$$M_R = \left|\frac{d-f_1}{f_2} + \left(\frac{1}{f_2} - \frac{d-f_1}{f_2^2}\right)s_2\right|$$

$$\tilde{s_2} = \frac{f_1 f_2}{f_1+f_2-d}\left(\frac{f_1}{f_2}\left|\frac{d-f_1}{f_2} + \left(\frac{1}{f_2} - \frac{d-f_1}{f_2^2}\right)s_2\right| + 1\right)$$

$$\tilde{s_1} = \frac{f_1 f_2}{f_1+f_2-d}\left(1 + \frac{1}{f_1}\frac{{f_2}^3}{|f_2(d-f_1)+(2f_2-d)s_2|}\right)$$

5 Literature

Abbe, E.: The Relation of Aperture and Power in the Microscope (continued). *Journal of the Royal Microscopical Society.* Volume 3, Issue 6. p. 790-812. December 1883.

Baumeister, W.: Electron tomography: towards visualizing the molecular organization of the cytoplasm. *Current Opinion in Structural Biology.* 12:679684. 2002.

Betzig, E., G.H. Patterson, R. Sougrat, O.W. Lindwasser, S. Olenych, J.S. Bonifacino, M.W. Davidson, J. Lippincot-Schwartz and H.F. Hess: Imaging Intracellular Fluorescent Proteins at Nanometer Resolution. *Science*, Volume 313, number 5793. p. 1642-1645. September 2006.

Born, M. and E. Wolf.: Principles of Optics (seventh (expanded) edition). The press syndicate of the university of Cambridge. Cambridge. 1999.

Garini, Y., B. J. Vermolen and I. T. Young: From micro to nano: recent advances in high-resolution microscopy. *Current Opinion in Biotechnology.* 16:3-12. 2005.

Hecht, E.: Optics (third edition). Addison Wesley Longman, Inc. New York. 1998.

Hell, S.W.:Toward fluorescence nanoscopy. *Nature Biotechnology*, Volume 21, number 11. p. 1347-1355. 2003.

Hess, S.T., T.P.K. Girirajan and M.D. Mason: Ultra-High Resolution Imaging by Fluorescence Photoactivation Localization Microschopy. *Biophysical Journal*, Volume 91, p. 4258-4272. December 2006.

Iijimaa, H., Y. Fukudab, Y. Araic, S. Terakawad, N. Yamamotoe and K. Nagayamab: Hybrid fluorescence and electron cryo-microscopy for simultaneous electron and photon imaging. *Journal of Structural Biology*, Volume 185, Issue 1. p. 107-115. January 2014.

Na Ji, N., H. Shroff, H. Zhong and E. Betzig: Advances in the speed and resolution of light microscopy. *Current Opinion in Neurobiology.* 18:605-616. 2008.

Reimer, L. and H. Kohl: Transmission Electron Microscopy: Physics of Image Formation (fifth edition). Springer Science+Business Media, LLC. New York. 2008.

Rust, M.J., M. Bates and X. Zhuang: Sub-diffraction-limit imaging by stochastic optical reconstruction microscopy (STORM). *Nature Methods*, Volume 3, number 10. p. 793-796. 2006.

Schermelleh, L., R. Heintzmann and H. Leonhardt: A guide to super-resolution fluorescence microscopy. *The Journal of Cell Biology*, Volume 190, number 2. p. 165-175. 2010.

Schindelin, J., I. Arganda-Carreras, E. Frise, V. Kaying, M. Longair, T. Pietzsch, S. Preibisch, C. Rueden, S. Saalfeld, B. Schmid, J. Tinevez, D.J. White, V. Hartenstein, K. Eliceiri, P. Tomancak and A. Cardona: Fiji: an open-source platform for biological-image analysis. *Nature Methods*, Volume 9, number 7, p. 676-682. July 2012.

Shroff, H., C.G. Galbraith, J.A. Galbraith and E. Betzig: Live-cell photoactivated localization microscopy of nanoscale adhesion dynamics. *Nature Methods*, Volume 5, number 5. p. 417-423. May 2008.

Taylor, J.R.: An Introduction to Error Analysis (second Edition). University Science Books. Sausalito. 1997.

Wang, Z.L.: Transmission Electron Microscopy of Shape-controlled Nanocrystals and Their Assemblies. *Journal of Physical Chemistry B*, Volume 104, number 6. p. 1153-1175. 2000.

Zhang, B., J. Zerubia and J.C. Olivo-Marin: Gaussian approximations of fluorescence microscope point-spread function models. *Applied Optics*, Volume 46, number 10. p. 1819-1829. April 2007.